

**Figure 3.**  $^{31}\text{P}$  MAS line width of PBFP during heating and cooling after annealing at 200 °C.

The temperature dependence of the  $^{31}\text{P}$  line width of the amorphous phase during the first heating cycle is shown in Figure 2. Note that the line width sharpens as more thermal energy enters the sample, except at temperatures just before the  $T(1)$  transition. The increase in the line width which occurs just before  $T(1)$  is reached is probably due to reorganization taking place before this transition. Cooling after the heating cycle results in an increase in the spectral line width that is measured at room temperature. During the second heating the spectral line width drops to a minimum value before peaking at approximately 75 °C, as compared to 50 °C that is observed for the first heating cycle. An enhancement of 3D ordering occurs upon cycling the sample as the results in Table I indicate.

$^{13}\text{C}$  MAS  $^1\text{H}$ -decoupled NMR spectra of PBFP obtained at 23 and 100 °C were almost identical except for a small decrease in line width of the single peak, which is consistent with the enhanced mobility of the  $\text{CH}_2$  portion of the side group in  $[-\text{N}=\text{P}(\text{OCH}_2\text{CF}_3)_2-]_x$ . As the sample passes through the  $T(1)$  transition it occupies a larger volume according to dilatometry results made on PBFP.<sup>5</sup> It therefore follows that the side chains have mobility even in the 3D phase of PBFP. The fluorine atoms on the end carbon atom split the signal into a quartet as anticipated from their chemical structure. Furthermore,  $^{13}\text{C}$  spin-lattice relaxation measurements made through  $T(1)$  for the  $\text{CH}_2$  and  $\text{CF}_3$  side groups on PBFP are 1.7 and 3.5 s, respectively. The corresponding activation energies associated with these groups are estimated to be  $E_{\text{CH}_2} \sim 17.3$  kJ/mol and  $E_{\text{CF}_3} \sim 13.7$  kJ/mol.

Since the upper temperature limit for in situ spinning in our Bruker spectrometer was limited to 100 °C, the PBFP sample was annealed at 200 °C outside of the instrument and slowly cooled to room temperature again. The  $^{31}\text{P}$  MAS NMR plot of line width versus temperature of this sample is shown in Figure 3. The spectral line width measured at room temperature is now much broader than it was before annealing. However, as the specimen temperature is increased stepwise in 10 °C intervals to 100 °C, the line width sharpens. This behavior is more pronounced (three to four times), but it is still consistent with the trend found before annealing. The increased line width observed at 30 °C is due to the inherently higher crystallinity, which now suppresses the mobility of the phosphorus-nitrogen backbone below  $T(1)$ . These results are in accord with the observations of Sun and Magill,<sup>3</sup> who found that annealing and thermal cycling of PBFP and other polyphosphazenes also increases their crystallinity. Solution  $^{31}\text{P}$  NMR was performed on the PBFP sample to determine if the chemical structure was altered due to annealing. A sharp singlet at -6.9 ppm before and after

annealing indicated that no chemical change had occurred.

In conclusion, these preliminary results serve to show that solid-state variable-temperature NMR is a useful technique that can be used to study in situ molecular chain dynamics, chain conformation, and specimen crystallinity, in accordance with the morphology of PBFP. Two distinct crystalline and amorphous regions are clearly exhibited by the chain backbone below  $T(1)$ . A single highly mobile ordered 2D phase exists above  $T(1)$ , in line with our other solid-state observations and properties. The  $-\text{OCH}_2\text{CF}_3$  side branches of the polymer exhibit mobility below the  $T(1)$  transition and appear to have a similar mobility and conformation on either side of the  $T(1)$  transition. The crystalline-amorphous ratio in PBFP assessed by solid-state NMR is strongly dependent upon annealing conditions and temperature of measurement.

**Acknowledgment.** We thank Professor George Marcelin for use of the NMR facilities, Dr. F. T. Lin for performing the solution NMR, and the National Science Foundation (Polymers Program, DMR 8509412) and the Office of Naval Research (Chemistry Division, N0001485K0358) for support of the work.

### References and Notes

- (1) Singler, R. E.; Schneider, N. S.; Hagnauer, G. L. *Polym. Eng. Sci.*, **1975**, *15*, 321.
- (2) Alcock, H. R. *Sci. Prog.* **1980**, *66*, 355.
- (3) Sun, D. C.; Magill, J. H. *Polymer* **1987**, *28*, 1243.
- (4) Kojima, M.; Magill, J. H. In *Morphology of Polymers*; Sedlacek, B., Ed.; Walter de Gruyter & Co.: New York, 1986.
- (5) Masuko, M.; Simeone, R. L.; Magill, J. H.; Plazek, D. J. *Macromolecules* **1984**, *17*, 2857.
- (6) Kojima, M.; Magill, J. H. *Makromol. Chem.* **1985**, *186*, 649.
- (7) Schneider, N. S.; Desper, C. R. In *Liquid Crystalline Order*; Blumstein, A., Ed.; Academic Press: New York, 1978; Chapter 9.
- (8) Ciora, R. J.; Sun, D. C.; Magill, J. H. *Proceedings Sixteenth North American Thermal Analysis Society*; Washington, DC, Sept 27-30, 1987; p 325.
- (9) Alexander, M. N.; Desper, C. R.; Sagalyn, P. L.; Schneider, N. S. *Macromolecules* **1977**, *10*, 721.
- (10) Crosby, R. C.; Haw, J. F. *Macromolecules* **1987**, *20*, 2324.
- (11) Tonelli, A. E.; Gomez, M. A.; Tanaka, H.; Schilling, F. C. *Polymer Prepr.* **1988**, *29*, 440.
- (12) Tanaka, H.; Gomez, M. A.; Tonelli, A. E.; Chichester-Hicks, S. V.; Haddon, R. C. *Macromolecules* **1988**, *21*, 2301.

† Also Materials Science and Engineering Department.

Scott G. Young and Joseph H. Magill\*†

School of Engineering, University of Pittsburgh  
Pittsburgh, Pennsylvania 15261

Received December 14, 1988;

Revised Manuscript Received March 6, 1989

### Polyethylene Crystallinity from Static, Solid-State NMR Spectra

It is well-known that linear polyethylene (LPE) rapidly crystallizes from the melt to form a semicrystalline solid with an amorphous phase and a crystalline phase. The interactions between these phases and the relative proportion of each phase are important factors affecting the bulk properties of the material.<sup>1</sup> A great deal of effort has been expended to accurately determine the crystallinity in semicrystalline polymers; the most common methods are X-ray diffraction, density measurement, differential scanning calorimetry (DSC), and  $^1\text{H}$  broad line NMR. High-resolution, cross-polarized, magic angle spinning (CP/MAS)  $^{13}\text{C}$  NMR can distinguish the crystalline phase

**Table I**  
Principal Elements of the Chemical Shielding Tensor of Polyethylene (ppm from TMS)

	2.35 T field		4.70 T field <sup>a</sup>		previous LPE <sup>7</sup>
	crystalline	amorphous	crystalline	amorphous	
$\sigma_{xx}$	51.1	40.2	50.1 (0.4)	39.6 (0.3)	51.4
$\sigma_{yy}$	33.9	36.4	34.0 (0.3)	36.3 (0.5)	38.9
$\sigma_{zz}$	15.5	13.7	15.2 (0.3)	12.6 (0.4)	12.9
$\sigma_{iso}$	33.5	30.1	33.1 (0.3)	29.5 (0.4)	34.4
TLB <sup>b</sup>	266	95	337 (47)	133 (38)	
measd crystallinity <sup>c</sup>		80%		82 (3)%	
correctd crystallinity <sup>d</sup>		73-77%		76-80%	

<sup>a</sup>The numbers reported here are the average of 10 independent measurements. The numbers in the parentheses are the standard deviation calculated from these 10 trials. <sup>b</sup>Given in hertz. This parameter is the total line broadening (full line width at half-height). Gaussian and Lorentzian line broadenings are so highly correlated that the error in each component greatly exceeds the error in the sum of the broadenings. This reflects the tensor simulation program's inability to differentiate precisely between Gaussian and Lorentzian broadenings. It is not informative to compare the total line broadenings obtained at the two field strengths because there are considerable sensitivity and  $B_1$  field homogeneity differences between the two probes. <sup>c</sup>The ratio of the integrated crystalline shielding tensor pattern to the total integrated intensity. <sup>d</sup>The percent crystallinity corrected for different cross-polarization efficiencies in the crystalline and amorphous regions (see text). Previous estimate of 73% for crystallinity by Phillips Petroleum Co. (private communication).

of LPE from the amorphous phase by utilizing differences in chemical shift<sup>2-4</sup> or relaxation times.<sup>4,5</sup>

A new method is proposed for determining the crystallinity of LPE by fitting the solid-state, <sup>1</sup>H-decoupled, CP static <sup>13</sup>C NMR spectrum with two different chemical shielding tensors, corresponding to the two different phases in the sample. One tensor represents the crystalline phase and one represents the amorphous phase. The ratio of the integrated crystalline tensor to the total integral (amorphous + crystalline) is taken as a good estimate of the crystallinity.

The sample was Phillips Petroleum Co. 6050 Fluff, a linear polyethylene whose crystallinity was estimated to be 73% from a calculation based upon X-ray data, which was calibrated with the measured density of the sample. The density of the sample was 0.960 g/cm<sup>3</sup> at 23 °C. The NMR experiments were conducted on a Bruker CXP-100 (2.35 T field), with a <sup>13</sup>C resonance frequency of 25.152 MHz. The temperature was 23 °C. The samples were placed in a static boron nitride rotor oriented perpendicular to the field. The pulse sequence used for this experiment is the common cross-polarization sequence with an 8.5- $\mu$ s 90° <sup>1</sup>H pulse, a 3-ms contact time, a 40-ms acquisition time, and a 3-s delay time between pulse sequences. The aliphatic peak of hexamethylbenzene (17.6 ppm downfield from TMS) was used as a chemical shift reference. The Fourier transformed spectra in Figure 1 were transferred to a VAX 11/750 computer for spectral simulation.

The POWDER fitting routine was used to fit the LPE spectra.<sup>6</sup> It computes the NMR powder pattern which most closely resembles the experimental data by varying parameters in a calculated spectrum until the sum of squares of deviations between the experimental spectrum and the calculated spectrum is minimized. The program's adjustable parameters include three principle values for each chemical shielding tensor, line broadening functions, and the ratio of the two integrated shielding tensors in the fit. All of the parameters in the fitting program are completely free to change; the criterion for completion of the fit is met when the difference between the sum of squares of deviations between two subsequent simulations is less than  $1.0 \times 10^{-5}$ .

Among the advantages of using a calculation program to fit static solid-state <sup>13</sup>C NMR chemical shielding patterns is the ability to discriminate subtle changes in the powder patterns in the vicinity of break points. This is especially true when the spectrum is fit with two tensors that have similar principal values and visual inspection is

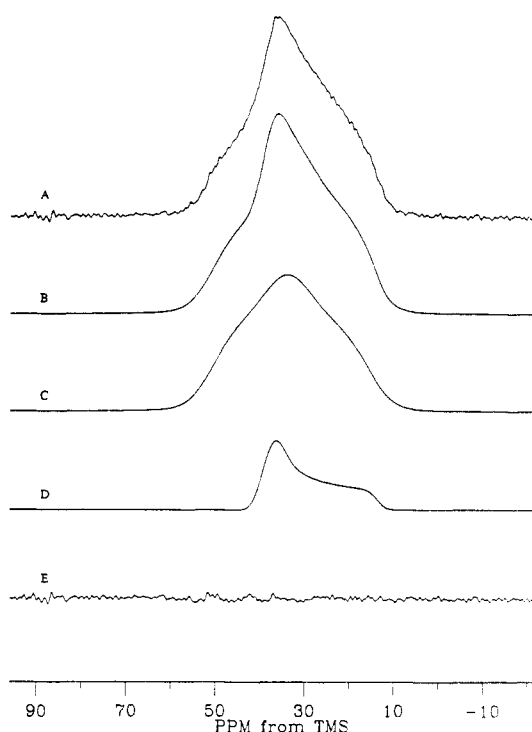


**Figure 1.** (A) Cross-polarized, <sup>1</sup>H-decoupled, static, 25.152-MHz <sup>13</sup>C NMR spectrum of Phillips 6050 fluff polyethylene. The spectral window was 5 kHz, no line broadening, 24 150 transients. (B) Calculated "best-fit" spectrum, the sum of the crystalline and the amorphous tensor components. (C) The crystalline tensor. (D) The amorphous tensor. (E) Residual spectrum (A - B). The chemical shifts are relative to the methyl resonance of hexamethylbenzene (17.6 ppm from TMS).

unable to distinguish small differences between the two shielding tensors.

The "best fit" for LPE is shown in Figure 1, and the shielding parameters of the fit are given in Table I. The ratio of the two chemical shielding tensors yields a crystallinity of 80%, which overestimates the crystallinity measured by Phillips by 7%. A possible source of error affecting this determination arises from differences in the cross-polarization efficiency between the crystalline and the amorphous phases of LPE. The crystalline phase consistently has a sensitivity enhancement factor of 3.5 compared to the 4-fold enhancement theoretically possible. The amorphous phase, however, typically cross polarizes less efficiently depending upon the sample due to increased molecular motion, resulting in sensitivity enhancements

of 2.4–3.0.<sup>3</sup> This correction results in a lower crystallinity. In the case of the present sample, the correction for cross-polarization efficiency yields a crystallinity between 73% and 77%, which is in reasonable agreement with the 73% value measured independently.

The diversity of line broadening functions from the "best fit" shown in Table I deserves comment. The amorphous tensor has a broadening of approximately 95 Hz (full line width at half-height), which is typical of single-crystal <sup>13</sup>C resonances and contains contributions from relaxation and incomplete decoupling. The crystalline tensor has an unusually large broadening of 266 Hz, which may reflect the additional dispersion caused by motional and conformational inhomogeneities at the interface of the crystalline domain of a semicrystalline sample in addition to the contributions described above. The same inhomogeneities may also exist in the amorphous region of the sample, but rapid motions occurring in this region could average the dispersion to give a line width more typical in a homogeneous sample.

In order to establish the reliability of this technique, the experiment was repeated with the same sample on a Bruker CXP-200 (4.70 T field) spectrometer, with a 3.9- $\mu$ s 90° <sup>1</sup>H pulse, a 3-ms contact time, a 26-ms acquisition time, a 5-s delay time between pulse sequences, and 2000 acquisitions. The statistical reproducibility of the shielding values and the crystallinity was then demonstrated by repeating this experiment 10 times. The resulting spectra were fit as described above, each with a different set of starting parameters to ensure that the path to convergence was different for each fit. The results of this test are tabulated along with the standard deviations in Table I.

An interesting sidelight to the determination of the crystallinity is the difference between the shielding tensors representing the two phases of LPE. The crystalline shielding tensor is asymmetric with three principal values representing the chemical shift along three orthogonal directions. The amorphous shielding tensor was found to be nearly axially symmetric and quite different from the crystalline tensor. This fact is difficult to explain in chemical terms because there is no chemical variation between the two phases of LPE. However, these phases do have different motional and conformational characteristics that can account for the different chemical shielding tensors.

The principal values of the <sup>13</sup>C chemical shielding tensor of LPE have been measured and assigned to the molecular axis, as shown in Figure 2.<sup>7,8</sup> Rapid anisotropic molecular reorientation about the polymer chain axis would leave  $\sigma_{zz}$  unchanged and would average the components perpendicular to the polymer chain axis; namely,  $\sigma_{xx}$  and  $\sigma_{yy}$ .<sup>9</sup> (Rapid meaning, e.g.,  $1/\tau_c \ll \|H_{\text{internal}}\| \sim 2$  kHz in this case.  $\tau_c$  is the correlation time of the motion and  $H_{\text{internal}}$  is the chemical shielding Hamiltonian.) Effective averaging to an axially or nearly axially symmetric chemical shielding tensor such as the one observed for the amorphous phase requires that the molecular reorientation equally samples orientations in the  $x$  and  $y$  directions of the molecular frame (see Figure 2). Intuitively, this type of motion is much more probable than motion occurring about an axis perpendicular to the polymer chain axis requiring large, end-over-end rotations of the polymer chain in order to average  $\sigma_{zz}$  with either  $\sigma_{xx}$  or  $\sigma_{yy}$ . Hence the motions required to produce the observed near axially symmetric tensor from the amorphous region of LPE are consistent with other experiments and models proposing segmental motions in the amorphous phase of LPE and other semicrystalline polymers.<sup>10,11</sup>

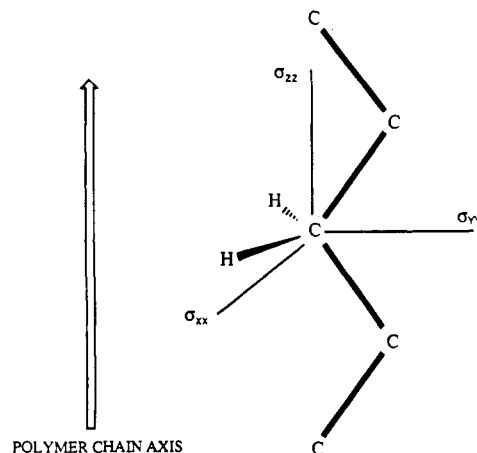


**Figure 2.** Chemical shift tensor of polyethylene in the molecular axis frame.  $\sigma_{xx}$  is parallel to the proton-proton internuclear vector,  $\sigma_{yy}$  is parallel to the H-C-H angle bisector, and  $\sigma_{zz}$  is parallel to the polymer chain axis.<sup>7,8</sup>

The isotropic values of the two chemical shielding tensors contain conformational information that distinguishes the crystalline phase from the amorphous phase of LPE. The conformation of the carbon-carbon bonds in the vicinity of a <sup>13</sup>C methylene group determines its chemical shift, hence the isotropic chemical shift reflects the relative contribution of the trans and gauche conformations to the overall conformation of the polyethylene chain. The crystalline phase of LPE has an exclusively all-trans conformation, resulting in an isotropic chemical shift of 33.5 ppm (see Table I). As the carbon bond conformations change from all trans, an upfield change in the chemical shift occurs, reaching its highest field position in the all-gauche conformation. Liquid cyclohexane is constrained in the all-gauche conformation, and its chemical shift of 27.84 ppm from TMS is taken as an estimate of the chemical shift of the all-gauche conformation of methylene groups in general.<sup>4</sup> The isotropic chemical shift of the amorphous phase of LPE is found 3.4 ppm upfield from the all-trans shift and confirms the presence of a significant equilibrium population of gauche carbon-carbon bonds. Assuming that the isotropic chemical shift is determined by a linear relationship between the chemical shifts of the all-trans and the all-gauche conformations, the equilibrium population of gauche conformation ( $f_g$ ) has been estimated to be 60% from the isotropic chemical shifts reported in Table I from the following relationship:

$$f_g = \frac{\delta(\text{crystalline}) - \delta(\text{amorphous})}{\delta(\text{crystalline}) - \delta(\text{cyclohexane})} 100\%$$

Thus, the isotropic chemical shift of the amorphous region of LPE provides an estimate of the fraction of gauche carbon-carbon bonds in that phase.

**Acknowledgment.** We are grateful for the many helpful comments and suggestions provided by Dr. G. C. Grey. We are indebted to Dr. R. H. Boyd for supplying the samples. We would also like to thank the Phillips Petroleum Co. and particularly Dr. F. Kokesh for providing the crystallinity of the sample. This work has been supported by the Department of Energy under Grant DE-FG02-86ER1350.

**Registry No.** PE, 9002-88-4.

## References and Notes

- Boyd, R. H. *Polymer* **1985**, *26*, 323.
- Ando, I.; Sorita, T.; Yamanobe, T.; Komoto, T.; Sato, H.; Deguchi, K.; Imanari, M. *Polymer* **1985**, *26*, 1864.

- (3) VanderHart, D. L.; Khoury, F. *Polymer* **1984**, *25*, 1589.
- (4) Earl, W. L.; VanderHart, D. L. *Polymer* **1979**, *12*, 762.
- (5) Axelson, D. E.; Mandelkern, L.; Popli, R.; Mathieu, P. *J. Polym. Sci., Polym. Phys. Ed.* **1983**, *21*, 2319.
- (6) Alderman, D. W.; Solum, M. S.; Grant, D. M. *J. Chem. Phys.* **1986**, *84*, 3717.
- (7) VanderHart, D. L. *Macromolecules* **1979**, *12*, 1232.
- (8) Opella, S. J.; Waugh, J. S. *J. Chem. Phys.* **1977**, *66*, 4919.
- (9) Mehring, M. *High Resolution NMR in Solids*; Springer-Verlag: Berlin, 1983; p 51.
- (10) Speiss, H. W. *Colloid. Polym. Sci.* **1983**, *261*, 193.
- (11) Boyd, R. H. *Polymer* **1985**, *26*, 1123.

**Craig D. Hughes, Naresh K. Sethi, Jay H. Baltisberger,  
and David M. Grant\***

*Department of Chemistry, University of Utah  
Salt Lake City, Utah 84112*

*Received November 10, 1988;*

*Revised Manuscript Received March 7, 1989*